Sensitivity of the NO_y budget over the United States to anthropogenic and lightning NO_x in summer

Y Fang[1, 2], A.M. Fiore[2], L.W. Horowitz[2], H. Levy II[2], Y Hu[3], A.G. Russell[3]

1 Atmospheric and Oceanic Sciences Program, Princeton University, NJ, 08540
2. Geophysical Fluid Dynamics Laboratory, Princeton, NJ, 08540
3. School of Civil and Environmental Engineering, Georgia Institute of Technology, GA, 30332

We examine the implications of new estimates of the anthropogenic and lightning nitrogen oxide (NO_x) sources for the budget of oxidized nitrogen (NO_y) over the United States in summer using a 3-D global chemical transport model (MOZART-4). In response to the EPA State Implementation (SIP) call, the U.S. anthropogenic NO_x emissions decreased by 23% in July in our 2004 inventory compared to the 1999 U.S. EPA National Emissions Inventory. We incorporate recent observation-based estimates for lightning NO_x by increasing the model source over northern mid-latitude continents (by a factor of 10) and the fraction emitted into the free troposphere (FT, from 80% to 98%). These NO_x source updates improve the simulation of NO_x and O_3, although a bias in the partitioning between HNO_3 and PAN compared to the INTEX-NA aircraft observations remains, suggesting gaps in the current understanding of upper tropospheric processes. Although the model captures the observed spatial pattern of nitrate deposition ($r = 0.75$), regional discrepancies between the model and observations suggest that the lightning flash frequency distribution needs improvement. We estimate that lightning contributes 27-43% of the FT NO_y export from the U.S. to the North Atlantic (through 67.5°W at 24-48°N) and 28-43% to the NO_y wet deposition over the United States, with the ranges reflecting different assumptions. The export and burden of NO_y respond less than proportionally to NO_x source changes while the NO_y deposition responds more than proportionally, due to the changes in NO_y partitioning and lifetime. We estimate a model NO_y export efficiency of 4-14% to the North Atlantic in the FT, within the range of previous plume-based estimates (3%-20%) and smaller than the 30% exported directly from the continental boundary layer. The increase in lightning NO_x decreases the fractional contribution of PAN to total NO_y export, increases the O_3 production in the northern extratropical FT by 33%, and reduces the OPE by 30%. If models underestimate the lightning NO_x source, they overestimate the background OPE in the FT and the fractional PAN contribution to NO_y export and, hence, the O_3 production downwind due to anthropogenic NO_x export. Better constraints on the lightning NO_x source are required to more confidently assess the impacts of anthropogenic emissions and their changes on air quality over downwind regions.

1. Introduction:

Nitrogen oxides ($NO_x = NO+NO_2$) play a key role in atmospheric chemistry [*e.g.*, *Seinfeld and Pandis*, 2006]. In the troposphere, NO_x contributes to the formation of ozone (O_3) and affects the oxidizing capacity of the atmosphere. Mainly released as NO from combustion, lightning and soil emissions, then quickly converted to NO_2, NO_x can further be oxidized to peroxyacetylnitrate (PAN), nitric acid (HNO_3), and other minor oxidation products. These products, together with NO_x, are collectively known as oxidized nitrogen (NO_y). Longer-lived NO_y, especially PAN and, to a lesser extent, HNO_3 have the potential to act as reservoirs for NO_x and contribute to O_3 production on global scale after export from the NO_x source region [*e.g.*, *Moxim et al*., 1996; *Liang et al.,* 1998; *Horowitz and Jacob*, 1999; *Li et al.,* 2002, 2004; *Parrish et al*., 2004; *Hudman et al.,* 2004; *Penkett, et al*, 2004; *Auvray et al*., 2005]. Deposition of NO_y compounds, mostly in the form of highly soluble HNO_3, provides an important source of nutrients for marine, freshwater and terrestrial ecosystems, influencing their productivity and thereby affecting the global carbon cycle [*Galloway et al.,* 2004; *Prentice et al.,* 2001; *Vitousek et al*., 1997]. Understanding the budget of NO_y is thus necessary to assess the environmental impacts of NO_x sources.

As a major source of anthropogenic NO_x (22% of global anthropogenic emissions in 2000) [*Olivier and Berdowski*, 2001], the United States has been actively controlling its summer time NO_x emissions for more than a decade. For example, the Environmental Protection Agency (EPA) NO_x State Implementation (SIP) Call in 1998 has led to a reduction of NO_x emissions from power plants by 50% in the eastern United States between 1999 and 2003, as confirmed with Continuous Emission Monitoring System

62 (CEMS) measurements on power plant stacks [*Frost et al.*, 2006]. Satellite based
63 observations of tropospheric NO_2 provide additional evidence of this decline in NO_x,
64 showing a consistent trend of 7% yr^{-1} decrease for 1996-2006 over the eastern United
65 States [*van der A. et al*., 2008]. *Stavrakou et al* [2008] further inferred a 4.3% yr^{-1}
66 decrease of NO_x emissions over the Ohio River Valley from 1997 to 2006 from the
67 tropospheric NO_2 column.

68 While anthropogenic NO_x sources account for around 60% of total U.S. NO_x
69 emissions [*Parrish et al.,* 2004], the lightning source is a major natural source in the free
70 troposphere and it is the least known one within the total atmospheric NO_x budget with a
71 best estimate of 5 Tg N yr^{-1} and an uncertainty range of 1-20 Tg N yr^{-1} [*Schumann and*
72 *Huntrieser,* 2007 and references therein]. According to recent work by *Ott et al*. [2007],
73 each flash of lightning in the several mid-latitude and subtropical thunderstorms they
74 studied produces 360-462 mol N on average as compared to 81 mol N $flash^{-1}$ generated
75 by the lightning parameterization in our model (described in Section 2). In addition,
76 *Pickering et al* [2006] suggest that a larger percentage of the total lightning NO_x source is
77 located in the free troposphere (FT) than proposed in their earlier work [*Pickering et al*.,
78 1998].

79 During summer 2004, NASA conducted the Intercontinental Chemical Transport
80 Experiment –North America (INTEX-NA) field campaign over North America [*Singh et*
81 *al*., 2006]. The comprehensive suite of species observed during the INTEX-NA
82 campaign, including NO_y species and O_3, presents a valuable opportunity to examine the
83 NO_y budget in light of the recent anthropogenic NO_x emission changes and the revised
84 estimates for lightning NO_x, and to investigate the implications for O_3. Several studies

85 have already utilized the INTEX-NA observations relevant to NO_y and O_3. *Singh et al*
86 [2007] examined the observed NO_y partitioning within the North American troposphere
87 and pointed out significant differences between observations and models as well as
88 among models, suggesting a need for additional studies with models incorporating the
89 new constraints on NO_x sources and chemistry provided by the INTEX-NA campaign.
90 *Hudman et al*. [2007] found that the INTEX-NA observations are consistent with a 22%
91 decrease in fossil fuel NO_x from 1999 in the U.S. National Emission Inventory and that
92 increasing lightning NO_x in the GEOS-Chem model by a factor of 4 over northern
93 hemisphere mid-latitude continents improved the match between simulated NO_y species
94 and observations. Applying these changes to both anthropogenic and lightning sources,
95 they found a higher dO_3/dCO ratio (0.47) within the North American outflow during
96 summer 2004 than the range from studies in early 1990s (consistent with the decreased
97 anthropogenic NO_x emissions), and North American NO_x emissions during summer 2004
98 enhanced the hemispheric tropospheric ozone burden by 12.4%, with comparable
99 contributions from fossil fuel and lightning (5–6%), but only 1% from biomass burning
100 emissions despite 2004 being a record fire year over Alaska and western Canada
101 [*Hudman et al*., 2009]. *Kaynak et al* [2008] reported a small impact from lightning NO_x
102 on maximum 8-h O_3 in surface air over the United States (less than 2 ppb in 71% of
103 cases) in summer 2004.
104 Here, we extend these studies by comparing the impacts of changes in
105 anthropogenic and lightning sources on the U.S. NO_y budget (with a focus on export and
106 deposition), as well as the implications for O_3 production and O_3 air quality. We use a
107 global 3-D model, Model of Ozone and Related Tracers (MOZART-4) [*Horowitz et al*.,

2003, 2007; *Emmons et al*. 2009]. We describe and evaluate our simulations in Sections 2 and 3. Then we analyze the tropospheric NO_y budget from the United States during the summer of 2004, examine the sensitivity of the NO_y budget to the reported anthropogenic NO_x emission change and to the new constraints on the lightning NO_x source, and estimate the NO_y export efficiency of the U.S. surface NO_x emissions to the North Atlantic in Section 4. The implications for O_3 production and O_3 air quality from the emission changes are discussed in Section 5. Conclusions are given in Section 6.

2. Model description

The Model of OZone and Related Tracers (MOZART) version 4 is updated from MOZART-2 [*Horowitz, et al*., 2003], as described by *Emmons et al* [2009]. The version we use here is based on that used by *Horowitz et al.* [2007] (including the recommended isoprene chemistry from their work based on observed alkyl nitrates during the INTEX-NA campaign), except for the anthropogenic and lightning NO_x sources as described below.

Briefly, the model resolution for this simulation is 1.9° latitude by 1.9° longitude, with 64 vertical levels. The driving meteorological fields are from the Global Forecast System and updated every three hours [*Horowitz et al.,* 2007]. The influx of O_3 from the stratosphere is prescribed by the SYNOZ technique (500Tg yr^{-1}) [*McLinden et al.,* 2000]. Convective mass fluxes are diagnosed by the model, using the shallow and mid-level convective transport formulation of *Hack* [1994] and deep convection scheme of *Zhang and MacFarlane* [1995]. Vertical diffusion within the boundary layer is based on the parameterization of *Holstlag and Boville* [1993]. Wet deposition is taken from the formulation described in *Brasseur et al.* [1998]. The monthly mean dry deposition

132 velocities are from *Horowitz et al* [2003] except for O_3 (taken from *Bey et al* [2001]) and
133 PAN (taken from a separate MOZART-4 simulation in which it was calculated
134 interactively to reflect the updates described by *Emmons et al*. [2009]). Global
135 anthropogenic, biomass burning, and natural emissions are based on the POET emission
136 inventory for 1997[*Oliver et al.,* 2003; http: //www.
137 aero.jussieu.fr/projet/ACCENT/POET.php], except for biogenic emissions of isoprene
138 and monoterpene, which are calculated interactively using Model of Emissions of Gases
139 and Aerosols from Nature (MEGAN v.0) [*Guenther et al*., 2006].
140 Over North America during summer 2004, we use biomass burning emissions
141 from *Turquety et al*. [2007] as described in *Horowitz et al*. [2007] and anthropogenic
142 surface emissions from the EPA National Emission Inventory (NEI99, version 3,
143 http://www.epa.gov/ttn/chief/net/1999inventory.html) in our standard simulation
144 (INTEX-NA99-LowLght in Table1). In order to simulate the reported NO_x emissions
145 reduction, we replace the NEI99 anthropogenic NO_x emissions over the United States
146 (including part of southern Canada and Mexico) with a new inventory for August 2004,
147 which we apply from May through August 2004. These anthropogenic NO_x emissions are
148 projected to 2004 based on the VISTAS 2002 U.S. emission inventory [*MACTEC*, 2005]
149 and combined with CEM data obtained from EPA. Figure 1 shows the spatial distribution
150 of the differences in surface NO_x emissions from the 1999 to 2004 inventories. Besides
151 the expected NO_x reductions in the northeastern United States and the Ohio River Valley
152 [*U.S. EPA*, 2005] due to regulations on NO_x emissions under the NO_x SIP call, we also
153 see NO_x reductions in southern California, which may reflect regulations on automobile
154 NO_x emissions there [*Frost et al.,* 2008] or an overestimate of NO_x emissions in the late

155 1990s (mostly from motor vehicles) [*Kim et al*., 2009]. The total July surface NO_x
156 emissions (which includes 0.1 Tg N from soil emissions) in the continental United States
157 decreases from 0.68 Tg N in 1999 to 0.52 Tg N in 2004, consistent with the sum of soil
158 and fuel emissions constrained by the INTEX-NA observations in *Hudman et al.* [2009].
159 To incorporate the recent advances in understanding of the vertical profile and
160 flash production efficiency of lightning NO_x [*Pickering et al*., 2006; *Ott et al.*, 2007], we
161 make several modifications to our parameterization. The estimated lightning flash
162 frequency and resulting NO_x emissions are parameterized by the scheme of *Price et al*.
163 [1997], with flash frequency determined by the maximum cloud top height, cloud-to-
164 ground (CG) and intracloud (IC) flash ratio determined as in *Price and Rind* [1993]. The
165 resulting model lightning NO_x source is 0.018 Tg N in July over the United States with a
166 mean nitrogen production of around 80 mol N $flash^{-1}$. These values are much lower than
167 those constrained by observations: total source of 0.27Tg N during July 1-Aug 15, 2004
168 [*Hudman et al*., 2007] and a flash production rate of around 500 mol N $flash^{-1}$ at mid-
169 latitudes [*Ott et al.*, 2007]. The underestimate of the lightning source likely contributes to
170 the model underestimate of the observed NO_x profile in the upper troposphere (section
171 3.2). The model simulated CG lightning frequency is biased low compared to that
172 observed by the National Lightning Detection Network (NLDN), especially over the
173 regions extending southwest from the Midwest to Texas (Figure 2a, 2b). However, our
174 flash lightning frequency over the United States is close to the annual mean distribution
175 from *Schumann and Huntrieser* [2007] in which they review 3 decades of global
176 lightning NO_x studies: strong lightning around the Gulf of Mexico (up to 6-9 flashes $km^{-2}month^{-1}$ in our model *vs.* up to 64 flashes $km^{-2}year^{-1}$ and over the Midwest (around 1-3
177

178 flashes $km^{-2}month^{-1}$ in our model *vs.* 8-32 flashes $km^{-2}year^{-1}$) [*Boccippio et al.*, 2001]. In
179 the model, the total lightning NO_x source can be adjusted by modifying the flash
180 frequency, the energy per flash, or the NO_x emitted per unit energy. We choose to
181 increase the NO_x emitted per unit energy over the mid-latitude continents in the northern
182 hemisphere (north of 25°N) by a factor of 10 to achieve a similar regional production
183 (0.27 Tg N from July 1 to Aug 15) as *Hudman et al* [2007]. This scaling increases the
184 average production rate from 80 to around 800mol $flash^{-1}$ over the United States, higher
185 than the 500 mol N $flash^{-1}$ value suggested by *Ott et al* [2007] which compensates for the
186 underestimated lightning flash frequency (Figure 2). Our adjusted lightning NO_x
187 emissions follow the flash distribution and maximize near the east coast and Florida
188 (Figure 2c). We further modify the vertical profile of lightning NO_x emissions based on
189 findings from *Pickering et al* [2006]. The new profile reduces the fraction of lightning
190 NO_x in the surface layers (0-1km) from 20% to 2% and redistributes the remainder
191 proportional to the original profiles over the range 2-16km (Figure 3). These adjustments
192 together improved the MOZART-4 profiles of NO_x, O_3 and HNO_3 compared to the
193 INTEX-NA observations (as shown in section 3).
194 Our base simulation with updated anthropogenic and lightning NO_x sources
195 (hereafter, referred as INTEX-NA04) is used to analyze the budget and mean export of
196 NO_y. Additional sensitivity simulations are described in Table 1. All simulations were
197 conducted from December 2003 through the INTEX-NA period (July-August, 2004) with
198 the U.S. emission inventory for INTEX-NA (NEI99 or NEI99 with 2004 anthropogenic
199 NO_x emission) and increased lightning NO_x, implemented from May 2004 to allow for a

two-month spin-up to capture changes in summertime continental boundary layer chemistry.

3. Model evaluation

We first evaluate the MOZART-4 simulations by comparing them with observations made on board the NASA DC-8 aircraft during INTEX-NA campaign [*Singh et al.,* 2006]. The coverage of this aircraft is regional and the observations on board are thus suitable for comparison with our global model. Our evaluation focuses on NO_y (NO_x, PAN and HNO_3) and other species (O_3, OH) closely related to the budget of NO_y and tropospheric O_3 chemistry. We also compare the simulated nitrate wet deposition during summer 2004 with that monitored by the National Atmospheric Deposition Program (NADP).

3.1 Boundary layer distributions

Here we focus on the INTEX-NA99 and INTEX-NA04 simulations (Table 1). Comparisons of selected species below 2 km in the eastern United States are presented in Figure 4. In general, we find that the changes in surface NO_x emission have little influence on the spatial correlation despite the spatially heterogeneous emission changes (Figure 1), with observed NO_y, O_3 and OH ($r > 0.5$, except for HNO_3, $r = 0.3$), but do affect the mean model bias (Figure 4): the mean NO_x and O_3 bias in the INTEX-NA04 simulation decrease from 153 ppt (30%) to 15 ppt (3%) and from 6 ppb (12%) to 2 ppb (4%). The apparent degradation of the spatial correlation for NO_x reflects one model grid cell (covering Ohio and Pennsylvania); ignoring that point yields equivalent correlations ($r= 0.55$) in both simulations. PAN is overestimated (by ~ 350 ppt in INTEX-NA99 and ~ 250 ppt in INTEX-NA04). This bias persists when we update all the VOC emissions

224 from the NEI99 to the 2004 inventory. The model underestimates HNO_3 (mean bias of -
225 37 pptv in INTEX-NA99 and -379 pptv in INTEX-NA04). The underestimate of HNO_3
226 and overestimate of PAN will likely cause an overestimate of NO_y export from the model
227 boundary layer (BL).

228 **3.2 Vertical distributions**

229 Figure 5 shows the mean profiles of different species within the eastern United
230 States for all the model simulations. In general, the factor of 10 increase in lightning NO_x
231 improves simulated NO_x, O_3 and HNO_3 in the free troposphere: the upper-tropospheric
232 NO_x underestimate decreases from 750 to 540 ppt, comparable to the results from
233 *Hudman et al*. [2007]; the O_3 discrepancy decreases to within 10 ppb; HNO_3 discrepancy
234 decreases to within 40 ppt above 6 km. The modeled OH and PAN are not notably
235 improved. OH in the upper troposphere is underestimated by the LowLght simulations by
236 around 50%; the lightning adjustment, while improving the OH prediction in the upper
237 troposphere, leads to an overestimate of OH in the mid-troposphere with a maximum bias
238 of 60%. PAN is overestimated by around 70 ppt in the mid troposphere and less than 30
239 ppt in the upper troposphere in the INTEX-NA04 and INTEX-NA99 simulations (mean
240 biases are both less than 20%). Further modification of the lightning NO_x profile to
241 produce more in the upper troposphere would improve the HNO_3 simulation but worsen
242 the PAN prediction, indicating other causes of the bias. As a check on the total NO_y
243 simulation, we add HNO_3, PAN and NO_x (the major NO_y species) from both model and
244 observations and find that they agree better than the individual species do. For example,
245 between 4 and 8 km, the sum of the major NO_y species agrees with observations to within
246 10% after the lightning adjustment. This comparison supports the idea that some

processes important for NO_y partitioning in the upper troposphere are missing in the model. *Hudman et al*. [2007] also found problems in HNO_3 and PAN, especially in the mid-upper troposphere, but their PAN was underestimated by ~30% in the upper troposphere, while their HNO_3 was twice the observed value; simply readjusting lightning will not fix that HNO_3 and PAN partitioning bias either. *Pinder et al.* [2009, personal communication] also found an NO_y partitioning problem as compared to observations when several chemical mechanisms (CB05, RACM2, SAPRC07, and GEOS-Chem) were applied in a box model. The bias persists after updating to the *Blitz et al* [2004] estimate for the acetone quantum yield (which is included in MOZART-4 [*Emmons et al.,* 2009]) and may reflect overestimates of radical sources and subsequent chemical cycling [*Henderson et al*., 2009]. For example, uncertainties in isoprene chemistry are known to affect PAN formation [e.g., *Emmerson and Evans*, 2009]. In our model, we use a 4% yield of isoprene nitrate production from the reaction of isoprene hydroxyperoxy radicals with NO, which best captures the boundary layer concentrations of organic nitrates and their correlation with ozone observed in INTEX-NA, however, many uncertainties remain [*Horowitz et al*., 2007]. The excess PAN relative to HNO_3 in the mid-troposphere in our model is likely to lead to an overestimate of the potential influence of the U.S. NO_x emissions on O_3 production and NO_y deposition in downwind regions.

3.3 Wet deposition of inorganic nitrate

We compare the total summer time inorganic nitrate (including nitric acid and aerosol nitrate) wet deposition from the INTEX-NA04 and INTEX-NA04-LowLght simulations with observations from National Atmospheric Deposition Program (NADP,

Figure 6). Both simulations are well correlated with observations (r = 0.75). The updated lightning NO_x source leads to a better match with observations over the central United States, but the uniform scaling causes excessive wet deposition along the east coast. In general, our factor of 10 increase of lightning already leads to an overestimate of the mean nitrate wet deposition compared to the NADP observations, so it is not likely that the lightning NO_x source is higher than the value we have now in our updated lightning simulation: 180 Gg N over the United States during July 2004. Rather, this reflects the problem with flash frequency distribution seen in Figure 2.

4 The NO_y budget over the United States in July 2004

4.1 Base case budget of NO_y over the United States

In this section, we discuss the chemical processing, deposition and export following the U.S. NO_x emissions in July, focusing on our base simulation (the INTEX-NA04 simulation). We define the contiguous U.S. boundary layer (BL) as the region extending horizontally from 24-48°N and 67.5-127.5°W, from the surface to about 800hPa (around 2km). We also define the contiguous U.S. total column (TC) to refer to the same horizontal region but vertically extending to about 200hPa. Hereafter, we refer to these lateral boundaries (up to 200hPa) as "walls", for example, the lateral boundary at 67.5ºW, 24-48 ºN, from the surface to 200 hPa is referred as the "east wall".

The TC and BL NO_y budgets are summarized in Table 2. Around 70% of the total emitted nitrogen is deposited and the remaining 30% of the emitted nitrogen is exported from the continental boundary layer laterally and vertically. This estimate for export efficiency of emitted nitrogen (30%) is at the high end of the 20-30% summer ratio in

293 previous Eulerian studies [*Levy et al.,* 1987; *Horowitz et al.*, 1998; *Liang et al*., 1998; *Li*
294 *et al*., 2004; *Parrish et al.*, 2004; *Pierce et al.,* 2007]. Raising the BL top from 800 to
295 730 hPa, to be comparable to these studies, we still find a higher value (27%), possibly
296 due to the model overestimate of BL PAN. Eulerian estimates are usually higher than
297 those estimated by using the NO_y-CO relationships sampled in the outflow plumes
298 downwind from the United States [e.g., *Hudman et al*., 2007; *Parrish et al.*, 2004; Li et
299 al., 2004; *Stohl et al*., 2002]. However, this difference does not necessarily mean the
300 budget estimate is inconsistent with the observations as discussed in Section 7.
301 Most of the NO_y exported from the BL is transported to the free troposphere
302 vertically (27% vs. 30% total). NO_2 and HNO_3 are the most abundant NO_y species
303 (HNO_3 accounts for more than 30%, while NO_2 accounts for more than 25% of the BL
304 NO_y burden) since PAN is thermally unstable in the BL. NO_2 and HNO_3 are also the
305 most abundant components contributing to NO_y exported from the U.S. BL (each
306 accounts for more than 30%, with PANs contributing over 10%).
307 Lightning NO_x accounts for almost 30% of the total U.S. NO_x source in July,
308 similar to that estimated from NLDN [*Kaynak et al*., 2008]. Around 80% of all emitted
309 NO_x in the U.S. TC over the United States is deposited and about 20% is exported (Table
310 2), consistent with the estimate by *Sanderson et al*. [2008]. Eastward export through the
311 east wall of the United States dominates the export from the TC (116 vs. 19 and 17 Gg N
312 exported through the north and south walls respectively; there is a 29 Gg N inflow
313 through the west wall in July). PANs contribute 50% and NO_x contributes 17% to the
314 NO_y species composing the eastward flux.

315 Figure 7 shows the NO_y flux through the east wall of the United States. Outflow
316 dominates the transport here except south of 30°N, where weak inflow into the United
317 States exist. This pattern reflects the dominance of the Bermuda High during July. Due to
318 the location of North American jet stream, a maximum eastward outflow is located
319 between 200hPa and 400hPa, centered at around 45ºN. Vertical profiles of the relative
320 contribution of major components of NO_y to this eastward flux in the INTEX-NA04
321 simulation are shown in Figure 8. Near the surface, HNO_3 is by far the largest component
322 of exported NO_y with a maximum contribution of more than 40%. Wet deposition
323 decreases the HNO_3 contribution with altitude from the surface to 600 hPa, and then its
324 contribution remains almost constant at 30% up to 300 hPa. PANs contribute most to the
325 exported NO_y above the boundary layer with a maximum contribution of more than 60%
326 located at around 500 hPa, reflecting their longer lifetime at the colder temperatures in
327 the free troposphere (FT). Above 500 hPa, the relative contribution of PANs decreases as
328 that of NO_x increases.

329 **4.2 Effects of recent anthropogenic NO_x emission reductions on the U.S. NO_y budget**
330 **and export to the North Atlantic**

331 We determine the effects of the NO_x emission reductions in response to the SIP
332 call on the budget of NO_y by comparing the INTEX-NA99 and the INTEX-NA04
333 simulations (Table 2). From INTEX-NA99 to INTEX-NA04, BL NO_x emissions decrease
334 by 23%. As a result, the NO_y burden within the BL decreases by 19% (Table 2, from 19
335 Gg N to 15 Gg N). Meanwhile, the net export of reactive nitrogen from the BL decreases
336 by 20%, while the total deposition form the BL decreases by 24% (Table 2). This
337 nonlinearity between NO_x emission changes and the response of the NO_y budget terms is

associated with changes in NO_y partitioning [*Liang et al.,* 1998]. As surface NO_x emissions decrease, PAN increases from 22% to 24% while HNO_3 decreases from 36% to 32% of the NO_y burden. A smaller contribution from HNO_3 (which is efficiently removed by dry and wet deposition) implies a longer NO_y lifetime (+5% in the BL) and hence a relative increase in the NO_y burden and export, resulting in a less-than-proportional reduction of these two terms. For the same reason, the deposition of NO_y decreases more than proportionally. Similar results occur for the TC over the United States (Table 2). Decreasing the U.S. anthropogenic NO_x emissions thus lowers the NO_y burden, NO_y deposition and NO_y export from the United States in summer, but decreases NO_y deposition more efficiently than the NO_y burden and export.

Decreasing anthropogenic NO_x emissions also reduces the eastward export through the east wall of the United States (Figure 7b), with the largest reduction near the surface around 42ºN and at 300 hPa at around 45ºN. The corresponding NO_y concentration changes along the east wall of the United States (not shown) have a similar pattern. Surface emissions thus have a strong potential to affect not only surface export, but also the free tropospheric eastward export north of 40ºN, consistent with the dominant export mechanism which is associated with frontal passages at this latitude [*e.g., Fang et al*., 2009; *Owen et al*., 2006; *Li et al.,* 2005; *Cooper el al.,* 2001, 2002; *Merrill et al*., 1996].

4.3 Impact of lightning NO_x on the U.S. export to the North Atlantic and deposition

Due to the lightning adjustment, the NO_x source to the FT over the United States increases by 77%, while the total deposition increases by 99% and the export increases by 53%. The less-than-linear variation of NO_y export and more-than-linear variation of

361 NO_y deposition compared to the source change reflect the partitioning change (the
362 contribution of HNO_3 increases and that of PANs decreases), consistent with our findings
363 from the anthropogenic emission sensitivity experiment in Section 5 (note the opposite
364 sign of the emission perturbations).

365 The lightning adjustment results in a different pattern of the eastward NO_y flux
366 change (Figure 7c) from that associated with anthropogenic emissions (Figure 7b), with
367 one maximum located around 400 hPa, centered at 42ºN. The PAN contribution changes
368 up to 10% in the FT in the lightning perturbation case while it is only about -2% in the
369 anthropogenic emission perturbation case (Figure 8) even though the NO_x emission
370 perturbations within the total column are similar in both experiments. If the adjusted
371 lightning were correct, this partitioning change implies the LowLght simulations would
372 likely overestimate the relative contribution of PAN to the total exported NO_y while
373 underestimating the absolute export of NO_y produced by lightning. Using the partitioning
374 simulated by the LowLght models would cause an overestimate of the impact of the U.S.
375 anthropogenic NO_x emission reductions on global and downwind O_3 air quality even with
376 good constraints on U.S. anthropogenic NO_x emissions.

377 Here we estimate the contributions from lightning NO_x sources to the total FT
378 eastward export, the largest export pathway for NO_y. For this estimate, we use the
379 INTEX-NA04 and INTEX-NA-LowLght simulations in which lightning NO_x changes by
380 an order of magnitude. The export change is not linear to the emission change, as the
381 export through the east wall increases from 74 to 106 Gg N (Table 3, +43%,) in July after
382 the lightning adjustment (which increases the total FT source by 77%, Table 3). We
383 assume that this change is only due to the lightning NO_x increase over the U.S. plus the

384 increase in the inflow through the west wall (from 24 to 30 Gg N, reflecting the lightning
385 NO_x increase imposed over all the northern hemisphere mid-latitude continents). We
386 bracket our estimate of the lightning contribution to the U.S. FT eastward fluxes using the
387 following two limits: A. the NO_y entering through the west wall blows directly across the
388 region and is exported through the east wall; B. the NO_y from the west wall is all
389 deposited within the United States. As shown in Table 4, the increase in lightning NO_x in
390 the FT thus contributes from 26 (scenario A) to 32 GgN (scenario B) to the total July
391 NO_y eastward export in the INTEX-NA04 simulation. The original lightning NO_x source
392 over the United States provides 14 Gg N during July. Thus upper and lower bound
393 assumptions of 0-100% deposition in this simulation yields a range of 14-0 Gg N
394 contribution from the original lightning to the July eastward export. Combining this range
395 with the range estimated above with enhanced export from the increased lightning yields
396 an estimate for the total lightning contribution of 26-46 Gg N, or 24-43% of the U.S. NO_y
397 export to the North Atlantic in the FT.

398 With similar assumptions, we estimate the contribution from lightning to the wet
399 deposition over the United States. Combining the lightning NO_x in the INTEX-NA04-
400 LowLght simulation (0-14 GgN) with the change of FT wet deposition to the INTEX-
401 NA04 simulation (96-102 Gg N), we estimate that lightning NO_x accounts for 96-116
402 GgN (47-57%) of total wet deposition from the FT. Since the lightning source within the
403 BL is only around 2% of the total BL NO_x emissions, we assume that its contribution to
404 wet deposition in the BL (134 GgN) is negligible and estimate the lightning NO_x
405 contribution to the total U.S. NO_y wet deposition to be 28-34%. Over remote regions, the
406 lightning NO_x contribution to total wet deposition may be much higher. Changes in

lightning activity may thus be detectable from measurements of nitrate deposition, particularly if subjected to nitrogen isotope analysis that can distinguish among anthropogenic and lightning sources [*Hastings et al*., 2003].

4.4 Export efficiency of U.S. surface NO_x emissions

Past work indicates that the Eulerian-based estimate of NO_y export efficiency may serve as an upper limit for the export out of the United States. *Hudman et al.* [2007] reported a NO_y export efficiency from the North American BL by focusing on the NO_y-CO relationships within anthropogenic plumes (we refer to this method "plume-based") between 2.5 and 6.6 km and found consistent values from the GEOS-Chem model (14±8%) and from observations (16±10%), lower than our Eulerian estimate (30%, Section 4) and that from Pierce et al [2004] (24%). Plume-based estimates of NO_y export efficiency are as low as 3% for export above 3 km for the 1996 and 1997 North Atlantic Regional Experiments (NARE) [*Stohl et al*., 2002]. The apparent discrepancies between the Eulerian and observed plume-based estimates reflect losses in NO_y occurring between export from the continental BL and arrival at the point sampled [*Parrish et al.*, 2004]. Indeed, *Li et al* [2004] demonstrate in the GEOS-Chem model that the Eulerian estimate (20%) is consistent with plume-based estimate of 15±10% for the 1997 NARE.

Rather than applying the plume-based approach, we use the lofted surface component of the FT (800-200hPa) eastward export of NO_y to determine the export efficiency to account for the export out of the United States to the downwind regions and to avoid additional wet depositions occurring within the United States being included into this export efficiency. Table 4 shows the contributions of different components to the total July FT NO_y eastward export in the INTEX-NA04 simulation. The eastward export

430 in the FT originating from the boundary layer ventilation is estimated to be 22-74 GgN
431 (out of the total surface emissions of 520 Gg N in July), yielding a 4-14 % range for the
432 FT export efficiency to the North Atlantic, with the range resulting from various
433 assumptions (see Section 4.3 and Table 4). This estimate is within the range of previous
434 plume-based estimates (3-20%, e.g., *Stohl et al*., 2002; *Parrish et al*., 2004; *Li et al.*,
435 2004; *Hudman et al*., 2007).

436 The accuracy of the plume-based export efficiency estimate depends on many
437 factors, such as the treatment of the background CO [*Li et al*., 2004] and the altitude of
438 the plumes sampled. Our approach provides an average view of the NO_y export efficiency
439 within the whole FT to the North Atlantic.

440 In addition, results from the anthropogenic sensitivity experiment (Section 4.2), in
441 which 157 Gg increases of anthropogenic emissions causes a 5 Gg N increases in the FT
442 eastward export (Table 2), suggests that the export efficiency from the increased
443 anthropogenic emission is 3%. However, this estimate is unlikely to represent the "real"
444 anthropogenic export efficiency due to the non-linearity discussed in section 4.2. Indeed,
445 the export efficiency of the total anthropogenic emissions should be greater than 3%. To
446 avoid the impact of non-linearity induced by emission perturbations from sensitivity
447 studies on the export efficiency calculation, a possible solution is to use "tag"
448 anthropogenic NO_x within the United States [*Horowitz et al*., 1999] and quantify its
449 contribution to the eastward NO_y export.

450

451 **5. Implications for O_3 production**

452 **5.1 O_3 production in the U.S. BL and in the northern hemispheric FT**

453 We examine the implications for O_3 production from the changes in
454 anthropogenic and lightning NO_x sources. Our simulations indicate that the 23% decrease
455 in surface NO_x emission from the 1999 to 2004 inventory decreases the gross O_3
456 production in the United States BL by 10%, from 17.0 to 15.3 G mol d^{-1}. The less-than-
457 proportional decrease reflects an increase in ozone production efficiency (OPE, from 19.1
458 to 23.9) [*Liu et al.*, 1987; *Lin et al*., 1988; *Jacob et al*., 1993; *Thompson et al* et al., 1994;
459 *Horowitz et al.,* 1998]. The OPE over the northeastern United States increases by around
460 20%, higher than the 9% estimate from *Hudman et al.* [2009], due to a larger NO_x
461 emission change in our experiment within this region (24%) relative to their work (15%).
462 The direct O_3 export out of the U.S. BL decreases by 0.55 Gmol d^{-1} (by 28% of the O_3
463 direct export), around 32% of the decrease in the gross O_3 production (1.7 Gmol d^{-1})
464 within the U.S. BL. This ratio is comparable to that found by *Li et al* [2004] when the
465 North American NO_x anthropogenic emissions were turned off. The decrease in FT O_3
466 production over the United States, due to decreased NO_y exported from the BL, is 0.4 G
467 mol d^{-1}, 73% of the direct O_3 export reduction from the U.S. BL.
468 The enhanced lightning NO_x increases gross O_3 production in the FT over the
469 United States by 49% (from 10.6 to 15.5 G mol d^{-1}). Meanwhile, the OPE is reduced by
470 46% (from 56.3 to 30.2). A previous study showed a mean FT OPE of 61 over the United
471 States [*Liang et al*., 1998], similar to our INTEX-NA04-LowLght simulation. The gross
472 O_3 production in the FT north of 30°N is 55.4 G mol d^{-1} in the INTEX-NA04-LowLght
473 simulation, also consistent with the estimate of *Wang et al.* [1998] (51 Gmol d^{-1}
474 annually). After increasing the lightning NO_x source in the INTEX-NA04 simulation, the
475 gross O_3 production within this region is enhanced to 73.7 G mol d^{-1} (+33%) with the

476 mean OPE reduced from 56 to 39 (-30%). We conclude that a model with a lightning
477 NO_x source biased low will overestimate the background OPE along with the relative
478 contribution of PAN to NO_y export, both of which may lead to an overestimate of the
479 contribution from anthropogenic NO_x emissions to O_3 in downwind regions even if the
480 anthropogenic emissions are well represented. Further efforts are needed to better
481 quantify the lightning NO_x source to obtain a more reliable evaluation of the impact of
482 anthropogenic NO_x emissions on global-scale O_3 production.

483 **5.2 Surface O_3 over the contiguous United States**

484 The anthropogenic NO_x emission reductions from 1999 to 2004 improve O_3 air
485 quality, especially in the eastern United States and California (Figure 9). July mean daily
486 maximum 8-h surface (MDA8) O_3 decreases by 9-12 ppbv in these two regions where
487 total O_3 is above 70 ppbv. The maximum decrease in MDA8 O_3 over the eastern United
488 States occurs to the south of the maximum NO_x emission change (over Kentucky,
489 Tennessee and Missouri, Figure 1), consistent with the results of *Hudman et al*. [2009]
490 and *Kim et* al. [2006]. Within the northeastern and mid-west United States, the monthly
491 mean MDA8 O_3 decreases by around 5-7 ppbv (comparable to 4-6 ppbv from *Hudman et*
492 *al* [2009] and 7 ppbv from *Kim et al* [2006]). Over Los Angeles, MDA8 O_3 increases
493 despite the decrease of NO_x emissions, likely reflecting the NO_x-saturated regime for O_3
494 production there. Decreases of the monthly mean 24-hour average surface O_3
495 concentrations show a similar pattern to MDA8 O_3, except the maximum change is lower
496 (6 ppbv). Stronger sensitivity of the MDA8 O_3 reflects the rapid photochemical
497 production fueled by local precursor emissions as compared to the complex nighttime
498 processes that affects the 24-hour average surface O_3 [*Russell et al*., 1986].

Surface O_3 concentrations are weakly affected by the adjustment to the northern hemispheric lightning NO_x source. The monthly mean MDA8 O_3 concentration increases by up to 3.5 ppbv, with the largest increase occurring to the northeast of Florida and to the east of California. In section 2, we mentioned that we scaled the lightning NO_x source by a factor of 10 in the NH mid-latitudinal continents and we also reduced the fraction of lightning NO_x in the surface layer from 20% to 2%. These adjustments counteract with each other, and therefore, lightning emission remains almost unchanged in the boundary layer. So surface O_3 change is mostly due to the lightning NO_x change in the FT. The maximum O_3 concentration change near Florida is associated with the maximum lightning NO_x emission change over Florida (Figure 2b). However, the lightning NO_x change corresponding to the maximum O_3 concentration change to the east of California is weak. In this region, subsidence of air dominates, bringing the lightning-influenced air parcels from the free troposphere to the surface over the western United States. This downward O_3 flux into the planetary boundary layer over western North America is also shown by *Parrington et al*.[2009]. The monthly mean 24-hour average surface O_3 shows both a similar pattern and similar magnitude (up to 3 ppbv) as that of MDA8 O_3, confirming that lightning NO_x affects surface O_3 through downward transport of free tropospheric air parcels, rather than through local photochemical production. In general, the lightning-induced surface O_3 concentration changes are small and not located in the most polluted regions, e.g., 8-h O_3 nonattainment regions at northeast corridor and California (http://www.epa.gov/air/oaqps/greenbk/map8hrnm.html), and therefore, the lightning adjustment has a relatively small impact on the typical maximum O_3 over those regions where it is of greatest concern [*Kaynak et al*., 2008]. However, it affects the

522 baseline level considered in setting the National Ambient Air Quality Standards
523 (NAAQS), termed the "Policy Relevant Background (PRB)" [*EPA*, 2006]. The
524 contribution from lightning to the surface O_3 can be as high as 3 ppbv over the western
525 United States and near Florida, about one tenth of previous surface O_3 background
526 estimates (15-45 ppb; highest in the western United States) [*Altshuller and Lefohn.*, 1996;
527 *Lin et al.*, 2000; *Jaffe et al*., 2003; *Fiore et al*., 2002, 2003; *Vingarzan.*, 2004], and
528 around 1 ppbv elsewhere.
529
530 **6. Conclusions**
531 Nitrogen oxides (NO_x) and their oxidation products affect the tropospheric O_3
532 budget and the oxidizing power of the atmosphere, as well as ecosystem productivity and
533 thereby the global carbon cycle. The U.S. anthropogenic NO_x emissions have decreased
534 since the mid-1990s, especially from 1999 to 2004 in response to the U.S. Environmental
535 Protection Agency (EPA) State Implementation (SIP) Call [*Kim et al*., 2006; *Stavrakou et*
536 *al*., 2008; *van der A et al*., 2008; *Frost et al.,* 2006]. In addition, recent work suggests that
537 lightning NO_x is higher than previously thought over the mid-latitudes of the northern
538 hemisphere and that the empirical vertical profile of lightning-produced nitrogen applied
539 in the current generation of CTMs needs revision [*Ott et al.,* 2008; *Pickering et al.,*
540 2006]. We use the MOZART-4 chemical transport model to examine the budget of NO_y
541 species in the United States during summer 2004 and investigate its sensitivity to these
542 changes in NO_x sources.
543 Our evaluation of the model with observations from INTEX-NA shows that using
544 the 2004 NO_x emission inventory versus the 1999 inventory (NEI99) reduces the mean

545 bias of the boundary layer (BL) simulation while maintaining the spatial correlations (r>
546 0.5 for most NO_y species). Scaling up the FT NO_x lightning emission by a factor of 10
547 improves the profiles of NO_x and O_3 relative to observations, but there is still a
548 considerable underestimate (60%) in the upper troposphere for NO_x. HNO_3 and PAN are
549 not notably improved in our model after the emission adjustments, indicating a bias in
550 chemical partitioning, as found in other models [*Singh et al*., 2007; *Pinder et al*., 2009,
551 personal communication], possibly reflecting uncertainties in isoprene chemistry [*e.g.,*
552 *Emmerson and Evan*, 2009] or the convection related processes that affect the upper
553 troposphere [*Bertram et al.,* 2007]. When the lightning NO_x is adjusted upward, the
554 spatial correlation of nitrate wet deposition between the model and the National
555 Atmospheric Deposition Program (NADP) observations is the same as in the base
556 simulation (r = 0.75); the total nitrate deposition simulation improves over the Midwest
557 and inland of southeast United States but worsens over the east coast (Figure 6).
558 We assessed the impact of the anthropogenic and lightning NO_x changes on U.S.
559 O_3 air quality. Anthropogenic NO_x emission reductions lower the monthly mean daily
560 maximum 8-h surface (MDA8) O_3 by up to 12 ppb over Kentucky, Tennessee, Missouri
561 and California, and by 5-7 ppb over Northeast Corridor and Midwest, consistent with
562 prior studies [*Hudman et al*., 2009; *Kim et al*., 2006]. The lightning impact on surface O_3
563 is weaker, especially over the highly polluted regions [*Kaynak et al.,* 2008], though it
564 does raise the Policy-Relevant-Background (PRB) O_3 (15-45 ppb over the United States,
565 with the highest levels in the west, e.g., *Fiore et al.,* 2003) by 3 ppbv over the western
566 United States and near Florida and 1 ppbv in other regions.

In our model, most NO_x emitted in July is removed by wet or dry deposition within the United States (~70% in the boundary layer, BL and 80% in the total column, TC), with the rest exported. The budget sensitivity analysis shows a more-than-proportional change of NO_y deposition and a less-than proportional change of NO_y export in response to the changing NO_x emissions, resulting from the NO_y partitioning and lifetime changes [e.g., *Liang et al*., 1998]. We estimated the range of lightning NO_x contribution to the total NO_y wet deposition over the United States and to the U.S. FT export to the North Atlantic to be 28-34% and 27-43% in the INTEX-NA04 simulation, respectively, with the range reflecting different assumptions.

We further calculate the range of the anthropogenic contribution to the U.S. FT export to the North Atlantic to be 22-74 GgN in July, yielding an estimate for NO_y export efficiency (the ratio of the anthropogenic export to the North Atlantic between 800 and 200 hPa over total U.S. surface NO_x emissions) of 4-14% (from 800 to 200hPa), with the high end consistent with plume-based estimates of NO_y export efficiency during the INTEX-NA campaign (14±8% in the GEOS-Chem model and 16±10% from the INTEX-NA observations between 2.5 km and 6.6 km [*Hudman et al.*, 2007]). This value is within the range of previous plume-based estimates and offers an alternative approach to estimating NO_y export efficiency from the traditional Eulerian budget and the plume-based analyses.

The adjustment to the lightning NO_x source increases the fractional contribution from HNO_3 to NO_y while decreasing that of PAN (Figure 8), suggesting that an underestimate of lightning NO_x would cause the relative PAN contribution to the total NO_y export to be overestimated. The Ozone Production Efficiency (OPE) in the FT over

590 the United States and the extra-tropical northern hemisphere decrease from 55 to 30 and
591 from 56 to 39, respectively, when lightning NO_x is increased. Even if anthropogenic
592 emissions are well represented, the overestimates of the fractional PAN contribution to
593 NO_y export and of northern hemispheric OPE can bias high the estimated impact of the
594 U.S. anthropogenic emission reduction on global and downwind O_3 air quality. Better
595 constraints on the lightning NO_x source are required to more confidently assess the
596 impacts of anthropogenic emissions and their changes on air quality over downwind
597 regions.

Acknowledgements

The authors would like to thank Rynda Hudman, Robert Pinder, Barron Henderson, Anand Ganadesikan and Emily Fischer for informative conversations, Rynda Hudman and Songmiao Fan for insightful review, the INTEX-NA campaign team for providing the NASA DC-8 aircraft observational data and the MOZART-4 development team.

References:

Altshuller, A. P., and A. S. Lefohn, Background ozone in the planetary boundary layer over the United States, J. Air Waste Management Assoc., 46, 134-141, 1996

Auvray, M., and I. Bey (2005), Long-range transport to Europe: Seasonal variations and implications for the European ozone budget, *J. Geophys. Res*., 110, D11303, doi: 10.1029/2004JD005503

Bey, I., D.J. Jacob, R.M. Yantosca, J.A. Logan, B.D. Field, A.M. Fiore, Q. Li, H.Y. Liu, L.J.Mickley, and M.G. Schultz (2001), Global modeling of tropospheric chemistry with assimilated meteorology: Model description and evaluation, *J. Geophys. Res.*, *106*, 23,073-23,095

Blitz, M. A., D. E. Heard, M. J. Pilling, S. R. Arnold, and M. P. Chipperfield (2004), Pressure and temperature-dependent quantum yields for the photodissociation of acetone between 279 and 327.5 nm, Geophys. Res. Lett., 31, L06111, doi:10.1029/2003GL018793

Boccippio, D. J., Cummins, K. L., Christian, H. J., and Goodman, S. J.: Combined satellite- and surface-based estimation of the intracloud-cloud-to-ground lightning ratio over the continental United States, Mon. Wea. Rev., 129, 108–122, 2001

Brasseur, G. P., D. A. Hauglustaine, S. Walters, P. J. Rasch, J.-F. Müller, C. Granier, and X. X. Tie (1998), MOZART, a global chemical transport model for ozone and related chemical tracers: 1. Model description, J. Geophys. Res., 103, 28,265–28,289

Cooper, O. R., J. L. Moody, D. D. Parrish, M. Trainer, J. S. Hplloway, T. B. Ryerson, G. Hubler, F. C. Fehsenfeld, S. J. Oltmans, and M. J. Evans (2001), Trace gas signatures of the airstreams within North Atlantic cyclones: Case studies from the North Atlantic Regional Experiment (NARE'97) aircraft intensive, J. Geophys. Res., 106, 5437–5456.

Cooper, O. R., J. L. Moody, D. D. Parrish, M. Trainer, J. S. Holloway, T. B. Ryerson, G. Hübler, F. C. Fehsenfeld, S. J. Oltmans, and M. J. Evans (2002), Trace gas composition of midlatitude cyclones over the western North Atlantic Ocean: A conceptual model, J. Geophys. Res., 107(D7), 4056, doi:10.1029/2001JD000901.

Emmerson, K. M. and Evans, M. J.: Comparison of tropospheric gas-phase chemistry schemes for use within global models, Atmos. Chem. Phys., 9, 1831-1845, 2009

Emmons, L. K., Walters, S., Hess, P. G., Lamarque, J.-F., Pfister, G. G., Fillmore, D., Granier, C., Guenther, A., Kinnison, D., Laepple, T., Orlando, J., Tie, X., Tyndall, G., Wiedinmyer, C., Baughcum, S. L., and Kloster, S., Description and evaluation of the Model for Ozone and Related chemical Tracers, version 4 (MOZART-4), Geosci. Model Dev. Discuss., 2, 1157-1213, 2009

EPA, Evaluating Ozone Control Programs in the Eastern United States: Focus on the NO_x Budget Trading Program, 2004

US Environmental Protection Agency, 2006, Air Quality Criteria for Ozone and Related Photochemical Oxidants (Final), Vols. I, II, and III. EPA 600/R-05/004aF-cF.

Fang, Y., A. M. Fiore, L. W. Horowitz, A. Gnanadesikan, H. Levy, Y. Hu, and A. G. Russell (2009), Estimating the contribution of strong daily export events to total pollutant export from the United States in summer, J. Geophys. Res., doi:10.1029/2008JD010946, in press

Fiore et al., A.M., D.J. Jacob, I. Bey, R.M. Yantosca, B.D. Field and A.C. Fusco, Background ozone over the United States in summer: origin, trend, and contribution to pollution episodes, Journal of Geophysical Research 107 (D15) (2002), p. 4275.

660 Fiore A.M., D.J. Jacob, H. Liu, Yantosca, T.D. Fairlie and Q. Li, Variability in surface ozone background
661 over the United States: implications for air quality policy, Journal of Geophysical Research 108 (D24)
662 (2003), p. 4787.
663
664 Frost et al. (2006), Effects of changing power plant NO_x emissions on ozone in the eastern United States:
665 Proof of concept, *J. Geophys. Res*., 111, D12306
666
667 Frost, G J, Kim, S, McKeen, S et al., (2008), Evaluating Texas NO_x emissions using satellite-based
668 observations and model simulations, Eos Trans. AGU, 89(53), Fall Meet. Suppl., Abstract A21B-0129
669
670 Galloway JN, Dentener FJ, Capone DG, Boyer EW, Howarth RW, Seitzinger SP, Asner GP, Cleveland CC,
671 Green PA, Holland EA, Karl DM, Michaels AF, Porter JH, Townsend AR, Vorosmarty CJ (2004) Nitrogen
672 cycles: past, present, and future. Biogeochemistry 70:153–226
673
674 Guenther, A., T. Karl, P. Harley, C. Wiedinmyer, P. I. Palmer, and C. Geron (2006), Estimates of global
675 terrestrial isoprene emissions using MEGAN (Model of Emissions of Gases and Aerosols from Nature),
676 Atmos. Chem. Phys., 6, 3181–3210
677
678 Hack, J. J., Parameterization of moist convection in the NCAR community climate model (CCM2), J.
679 Geophys. Res., 99, 5551–5568, 1994
680
681 Holtslag, A., and B. Boville, Local versus nonlocal boundary-layer diffusion in a global climate model, J.
682 Clim., 6, 1825–1842, 1993
683
684 Hastings, M. G., D. M. Sigman, and F. Lipschultz, Isotopic evidence for source changes of nitrate in rain at
685 Bermuda, J. Geophys. Res., 108(D24), 4790, doi:10.1029/2003JD003789, 2003.
686
687 Henderson Barron, R. Pinder, W. Goliff, et al., The role of chemistry in upper troposphere NO_2
688 underpredictions, http://www.cmascenter.org/conference/2009/slides/henderson_role_chemistry_2009.pdf
689
690 Horowitz et al. (1998), Export of reactive nitrogen from North America during summertime, *J. Geophys.*
691 *Res*., 103, 13,451-13,476.
692
693 Horowitz, L., and D. Jacob (1999), Global impact of fossil fuel combustion on atmospheric NOx, *J.*
694 *Geophys. Res*., 104(D19), 23823-23840
695
696 Horowitz, L. W., et al., A global simulation of tropospheric ozone and related tracers: Description and
697 evaluation of MOZART, version 2, *J. Geophys. Res*., 108(D24), 4784, doi:10.1029/2002JD002853, 2003.
698
699 Horowitz et al. (2006), Observational constraints on the chemistry of isoprene nitrates over the eastern
700 United States, *J. Geophys. Res*, 112, D12S08. doi:10.1029/2006JD007747, 2007
701
702 Hudman, R. C., et al. (2004), Ozone production in transpacific Asian pollution plumes and implications for
703 ozone air quality in California, J. Geophys. Res., 109, D23S10, doi:10.1029/2004JD004974.
704
705 Hudman, R. C., et al. (2007), Surface and lightning sources of nitrogen oxides over the United States:
706 magnitudes, chemical evolution, and outflow?, *J. Geophys. Res*., doi:10.1029/2006JD007912
707
708 Hudman, R. C., L. T. Murray, D. J. Jacob, S. Turquety, S. Wu, D. B. Millet, M. Avery, A. H. Goldstein, and
709 J. Holloway (2009), North American influence on tropospheric ozone and the effects of recent emission
710 reductions: Constraints from ICARTT observations, J Geophys Res, 114, D07302.
711
712 Jacob, D.J., Logan, J.A., Gardner, G.M., Yevich, R.M., Spivakovsky, C.M., Wofsy, S.C., Sillman, S. and
713 Prather, M.J., 1993. Factors regulating ozone over the United States and its export to the global atmosphere.
714 *Journal of Geophysical Research ,* 98 D8, pp. 14817–14826.
715

716 Jaffe, D.A., Parrish, D., Goldstein, A., Price, H. and Harris, J., 2003. Increasing background ozone during
717 spring on the west coast of North America. *Journal of Geophysical Research* **30** 12, p. 1613
718 (doi:10.1029/2003GL017024)
719
720 Kaynak, B., Hu, Y., Martin, R.V., et al., The effect of lightning NO_x production of surface ozone in the
721 continental United States, *Atmos. Chem. Phys*., 8, 5,151-5,129, 2008
722
723 Kim, S.-W., A. Heckel, S. A. McKeen, G. J. Frost, E.-Y. Hsie, M. K. Trainer, A. Richter, J. P. Burrows, S.
724 E. Peckham, and G. A. Grell (2006), Satellite-observed U.S. power plant NOx emission reductions and
725 their impact on air quality, Geophys. Res. Lett., 33, L22812, doi:10.1029/2006GL027749.
726
727 Kim, S.-W., A. Heckel, G. J. Frost, A. Richter, J. Gleason, J. P. Burrows, S. McKeen, E.-Y. Hsie, C.
728 Granier, and M. Trainer (2009), NO_2 columns in the western United States observed from space and
729 simulated by a regional chemistry model and their implications for NOx emissions, J. Geophys. Res., 114,
730 D11301, doi:10.1029/2008JD011343
731
732 Levy II, Hiram, and Walter Moxim, 1987: Fate of US and Canadian combustion nitrogen emissions.
733 Nature, 328(6129), 414-416
734
735 Li, Q., D. J. Jacob, I. Bey, P. I. Palmer, B. N. Duncan, B. D. Field, R. V. Martin, A. M. Fiore, R. M.
736 Yantosca, D. D. Parrish, P. G. Simmonds, and S. J. Oltmans, Transatlantic transport of pollution and its
737 effects on surface ozone in Europe and North America, *J. Geophys. Res*., *107*(D13), 4166,
738 doi:10.1029/2001JD001422, 2002.
739
740 Li et al. (2004), Export of NO_y from the North American Boundary Layer: Reconciling Aircraft
741 Observations and Global Model Budgets*, J. Geophys. Res*., 109, D02313, 10.1029/2003JD004086.
742
743 Li, Q., Jacob, D., Park, R., Wang, Y., Heald, C., Hudman, R.,Yantosca, R., Martin, R., and Evans, M.: North
744 American pollution outflow and the trapping of convectively lifted pollution by upper-level anticyclone, *J.*
745 *Geophys. Res*., 110(D10), 301,doi:10.1029/2004JD005039, 2005.
746
747 Liang et al. (1998), Seasonal budgets of reactive nitrogen species and ozone over the United States, and
748 export fluxes to the global atmosphere*, J. Geophys. Res*., 103, 13,435–13,450.
749
750 Lin, X., Trainer, M. and Liu, S.C., 1988. On the nonlinearity of the tropospheric ozone production. Journal
751 of Geophysical Research 93D, pp. 15839–15888
752
753 Lin, C.-Y.C., Jacob, D.J., Munger, J.W. and Fiore, A.M., 2000. Increasing background ozone in surface air
754 over the United States. *Geophysical Research Letters* 27, pp. 3465–3468
755
756 Liu et al. (1987), Ozone production in the rural troposphere and the implications for regional and global
757 ozone distribution, *J. Geophys. Res.*, 92, 4191-4207
758
759 MACTEC: Documentation of the revised 2002 base year, revised 2018 and initial 2008 emission
760 inventories for vistas, Visibility Improvement States and Tribal Association of the Southeast (VISTAS),
761 2005
762
763 McLinden, C. A., S. C. Olsen, B. Hannegan, O. Wild, M. J. Prather, J. Sundet, Stratospheric ozone in 3-D
764 models: A simple chemistry and the cross-tropopause flux, *J. Geophys. Res.,* 105(D11), 14653-14666,
765 10.1029/2000JD900124, 2000
766
767 Merrill., J. T. and J. L. Moody, Synoptic meteorology and transport during the North Atlantic Regional
768 Experiment (NARE) intensive: Overview, JGR, 101, 28903-28921, 1996
769
770 Moxim et al. (1996), simulated global tropospheric PAN: its transport and impact on NOx, ,
771 *J.Geophys.Res*., 101,12621-12638

National Atmospheric Deposition Program (NRSP-3). 2010. NADP Program Office, Illinois State Water Survey, 2204 Griffith Dr., Champaign, IL 61820.

Olivier, J., J. Peters, C. Granier, G. Pétron, J. F. Müller, and S. Wallens (2003), Present and future surface emissions of atmospheric compounds, POET Rep. 2, EU Proj. EVK2-1999-00011.

Olivier, J.G.J. and J.J.M. Berdowski (2001), Global emissions sources and sinks, In: The Climate System, edited by Berdowski, J., Guicherit, R.and B.J. Heij, pp. 33-78, A.A. Balkema Publishers/Swets , Zeitlinger Publishers, Lisse, The Netherlands.

Ott, L. E., Pickering, K. E., Stenchikov, G. L., Huntrieser, H., and Schumann, U.: Effects of lightning nox production during the 21 july european lightning nitrogen oxides project storm studied with a three-dimensional cloud-scale chemical transport model, J. Geophys. Res., 5075,112, D05307, doi:10.1029/2006JD007365, 2007.

Owen, R. C., O. R. Cooper, A. Stohl, and R. E. Honrath (2006), An analysis of the mechanisms of North American pollutant transport to the central North Atlantic lower free troposphere, J. Geophys. Res., 111, D23S58, doi:10.1029/2006JD007062.

Parrington, M., D. B. A. Jones, K. W. Bowman, A. M. Thompson, D. W. Tarasick, J. Merrill, S. J. Oltmans, T. Leblanc, J. C. Witte, and D. B. Millet (2009), Impact of the assimilation of ozone from the Tropospheric Emission Spectrometer on surface ozone across North America, Geophys. Res. Lett., 36, L04802, doi:10.1029/2008GL036935.

Parrish, D. D. (2004), Fraction and composition of NO_y transported in air masses lofted from the North American continental boundary layer, *J Geophys Res*, *109*, D09302, doi:10.1029/2003JD004226.

Penkett et al. (2004), Long-range transport of ozone and related pollutants over the North Atlantic in spring and summer, *Atmos. Chem. Phy*s. Discuss., 4, 4407– 4454.

Pickering, K. E., Y. Wang, W.-K. Tao, C. Price, J.-F. Müller (1998), Vertical distributions of lightning NOx for use in regional and global chemical transport models, *J. Geophys. Res.,* 103(D23), 31203-31216, 10.1029/98JD02651.

Pickering, K.E., Ott, L.E. DeCaria, A J ., et al. (2006) Using Results from Cloud-resolving Models to Improve Lightning NO_x Parameterizations for Global Chemical Transport and Climate Models, AGU 2006 Joint Assembly

Pierce, R. B., et al. (2007), Chemical data assimilation estimates of continental U.S. ozone and nitrogen budgets during the Intercontinental Chemical Transport Experiment–North America, J. Geophys. Res., 112, D12S21, doi:10.1029/2006JD007722.

Prentice, I.C., G.D. Farquhar, M.J.R. Fasham, M.L. Goulden, M. Heimann, V.J. Jaramillo, H.S. Kheshgi, C. Le Quéré, R.J. Scholes, and D.W.R. Wallace, The Carbon Cycle and Atmospheric Carbon Dioxide, in: Climate Change 2001: The Scientific Basis edited by J.T. Houghton, Y. Ding, D.J. Griggs, M. Noguer, P.J.v.d. Linden, X. Dai, K. Maskell, and C.A. Johnson,, pp. pp. 881 p, Cambridge University Press, Cambridge, United Kingdom and New York, NY, US, 2001., 2001.

Price, C., J. Penner, and M. Prather (1997), NOx from lightning 1. Global distribution based on lightning physics, J. Geophys. Res., 102(D5), 5929-5941

Price, C., and D. Rind (1993), What determines the cloud-to-ground lightning fraction in thunderstorms?, Geophys. Res. Lett., 20(6), 463-466

Ren, X et al. (2008), HO_x chemistry during INTEX-A 2004: observation, model calculation, and

comparison with previous studies, *J. Geophys. Res*., 113, D05310, doi:10.1029/2007JD009166

Russell, A. G., Cass, G. R., and Seinfeld, J. H.: On some aspects of nighttime atmospheric chemistry, Environ. Sci. Technol., 20, 1167–1172, 1986.

Sanderson, M. G., et al. (2008), A multi-model study of the hemispheric transport and deposition of oxidised nitrogen, Geophys. Res. Lett., 35, L17815, doi:10.1029/2008GL035389.

Schumann U. and Huntrieser, H.: The global lightning-induced nitrogen oxides source, Atmos.Chem. Phys., 7, 3823–3907, 2007

Seinfeld, J.H.; Pandis, S.N. Atmospheric Chemistry and Physics; Wiley: New York, 2006

Singh, H. B., W. Brune, J. Crawford, and D. Jacob (2006), Overview of the summer 2004 Intercontinental Chemical Transport Experiment-North America (INTEX-NA), *J. Geophys. Res*., doi:10.1029/2006JD007905

Singh, H. B., et al. (2007), Reactive nitrogen distribution and partitioning in the North American troposphere and lowermost stratosphere, *J. Geophys. Res.,* 112, D12S04, doi:10.1029/2006JD007664.

Stavrakou, T., J.-F. Müller, K. F. Boersma, I. De Smedt, and R. J. van der A (2008), Assessing the distribution and growth rates of NOx emission sources by inverting a 10-year record of NO2 satellite columns, Geophys. Res. Lett., 35, L10801, doi:10.1029/2008GL033521

Stohl, A., M. Trainer, T. B. Ryerson, J. S. Holloway, and D. D. Parrish, Export of NOy from the North American boundary layer during 1996 and 1997 North Atlantic Regional Experiments, J. Geophys. Res., 107(D11), 4131, doi:10.1029/2001JD000519, 2002

Thompson et al. (1994), Convective Transport over the central United States and its role in regional CO and ozone budgets*, J. Geophys. Res.,* 99(D9), 18703-18711

Turquety, S., et al. (2007), Inventory of boreal fire emissions for North America in 2004: Importance of peat burning and pyroconvective injection, J. Geophys. Res., 112, D12S03, doi:10.1029/2006JD007281.

van der A, R. J., H. J. Eskes, K. F. Boersma, T. P. C. van Noije, M. Van Roozendael, I. De Smedt, D. H. M. U. Peters, and E. W. Meijer (2008), Trends, seasonal variability and dominant NOx source derived from a ten year record of NO2 measured from space, J Geophys Res, 113, D04302, doi:10.1029/2007JD009021.

R. Vingarzan, A review of surface ozone background levels and trends, Atmospheric Environment 38 (21) (2004), pp. 3431–3442

Vitousek, P.M., J.D. Aber, R.W. Howarth, G.E. Likens, P.A. Matson, D.W. Schindler, W.H. Schlesinger, and D.G. Tillman, Human alteration of the global nitrogen cycle: Sources and consequences, *Ecological Applications*, *7* (3), 737-750, 1997.

Wang, Y., J. A. Logan, and D. J. Jacob (1998), Global simulation of tropospheric O_3-NO_x-hydrocarbon chemistry 2. Model evaluation and global ozone budget, *J. Geophys. Res.,* 103(D9), 10,727–10,755.

Zhang, G. J., and N. A. McFarlane, Sensitivity of climate simulations to the parameterization of cumulus convection in the Canadian climate centre general circulation model, Atmos. Ocean, 33, 407–446, 1995

878 **Table Captions**

879 **Table 1.** The U.S. NO_x emissions for July 2004 in the MOZART-4 simulations
880
881 **Table 2.** July Budget of NO_y species in the U.S (24-48º N, 127.5-67.5ºW) boundary layer
882 (BL, surface to 800 hPa) and the total column (TC, surface to 200 hPa) (unit: Gg N) in
883 the INTEX-NA04 simulation (values shown in each cell represent BL/TC values)
884
885 **Table 3.** July budget of NO_y species in the U.S. (24-48ºN, 127.5-67.5ºW) free
886 troposphere (FT, 800-200hPa)[1] (unit: Gg N)
887
888 **Table 4.** Contribution from different components to the total free troposphere (FT) U.S.
889 NO_y export to the North Atlantic in the INTEX-NA04 simulation during July, 2004 (unit:
890 Gg N)
891

892 **Figure Captions**

893 **Figure 1.** NO_x surface emission change (including anthropogenic and soil emissions).
894 The continental United States boundaries, 24-48ºN, 67.5-127.5ºW, are shown as black
895 dashed lines. Negative value indicates emission decreases from 1999 to 2004
896
897 **Figure 2.** The NLDN observed Cloud-to-ground (CG) flash frequency (a, top), the
898 MOZART-4 simulated CG flash frequency (b, middle) and the lightning NO_x source after
899 adjusting by a factor of 10 to better match the observational constraints (c, bottom) over
900 the contiguous United States (24-48ºN, 67.5-127.5ºW) during July, 2004
901
902 **Figure 3.** Vertical profiles used for allocating the lightning NO_x source in the INTEX-
903 NA-LowLght (black) and INTEX-NA (blue) simulations (see Table 1 and Section 2 for
904 details).
905
906 **Figure 4.** Modeled versus observed concentrations of selected species below 2 km in the
907 eastern United States during INTEX-NA period from the INTEX-NA99 simulation (red)
908 and from the INTEX-NA04 simulation (blue). Model results are sampled every minute
909 along the NASA DC-8 flight tracks in the eastern United States, and then both
910 observations (1 minute average) and model results are averaged onto the model grid.
911 Observations shown from NASA DC-8 are NO_x(a)[calculated as NO + NO_2, PI, *D. Tan*,
912 Georgia Institute of Technology], O_3(b)[PI, *M. Avery*, NASA LaRC], PAN(c)[*Singh*,
913 2007], HNO_3(d)[PI, R. Talbot, University of New Hampshire] and OH(e)[*Ren et al*.,
914 2008]; the organic correlation slopes of the INTEX-NA99 and INTEX-NA04 model
915 simulations are shown as red and blue lines respectively; the black line indicates a line
916 with a 1:1 slope; here and after, to account for the recent corrections to ATHOS absolute
917 calibration [*Ren et al*., 2008], the observed OH was scaled up by a factor of 1.64 for
918 comparison with our model.
919

Figure 5. Mean vertical profiles of NO_x (a), O_3 (b), PAN (c), HNO_3 (d), OH (e), and the major NO_y species (f, NO_x, PAN and HNO_3) during the INTEX-NA campaign in July-Aug 2004. Observations from the DC-8 aircraft (black) are compared with the INTEX-NA99-LowLght (red), INTEX-NA04-LowLght (blue), INTEX-NA99 (green) and INTEX-NA04 (orange) simulations. Horizontal bars show the standard deviations of each data set within each 2km layer. Simulated concentrations are sampled every minute along all the flight tracks for comparison with the observations. Both observation and models are then averaged within each horizontal model grid in 2 km altitude bins, and finally these gridded data are averaged (weighted by area) in each layer to get regional mean profiles

Figure 6. Inorganic nitrate wet deposition (unit: 10^{-1} g N m^{-2}) over the United States (June-August, 2004) from observations (left) and from the INTEX-NA04-LowLght (middle) and INTEX-NA04 (right) simulations (r = 0.75 between model and observed values in both simulations)

Figure 7. Latitudinal pressure section of NO_y fluxes (unit: 10^{-14} moles N sec^{-1} cm^{-2}) in the INTEX-NA04 simulation (a, top), changes in NO_y fluxes (unit: 10^{-14} moles N sec^{-1} cm^{-2}) through the east wall (67.5ºW) due to the anthropogenic emission regulations (b, middle, fluxes from INTEX-NA04 minus that from INTEX-NA99) and due to lightning adjustment (c, bottom, INTEX-NA04 minus INTEX-NA04-LowLght) through a wall at 67.5ºW, between 24 and 48 ºN during July, 2004; positive values indicate eastward fluxes while negative values indicate westward fluxes.

Figure 8. Relative contribution of the major NO_y components to the total NO_y flux through the east wall (67.5ºW, from 24-48ºN) of the United States in the INTEX-NA04 (open circles), the INTEX-NA99 (stars), the INTEX-NA04-LowLght (filled circles) simulations. Simulations are described in Table 1.

Figure 9. Monthly mean MDA8 O_3 concentration change due to decreases in the U.S. anthropogenic NO_x emissions (top, only land-boxes are shown) and due to increases in lightning NO_x (bottom) (unit: ppbv)

Tables

Table 1. The U.S. NO_x emissions for July 2004 in the MOZART-4 simulations

NO_x Emissions (Gg N)	INTEX-NA99-LowLght[1,2]	INTEX-NA99[1,4]	INTEX-NA04[3,4]	INTEX-NA04-LowLght[2,3]
Surface[5]	680	680	520	520
Vertically distributed[6]	38	200	200	38

[1] NEI99 emissions as in *Horowitz et al.* [2007]

[2] Original lightning NO_x source, distributed according to Pickering et al. [1998] (black line in Figure 3)

[3] Anthropogenic surface NO_x emissions updated to 2004 as described in Section 2

[4] Updated lightning NO_x sources, scaled up by a factor of 10 over northern hemispheric mid-latitude continents with a modified vertical distribution (blue line in Figure 3)

[5] Surface emissions include soil (0.1Gg N) and anthropogenic emissions

[6] Vertically distributed NO_x source includes biomass burning and aircraft (together 0.02 Gg N) and lightning

965 **Table 2.** July Budget of NO_y species in the U.S (24-48º N, 127.5-67.5ºW) boundary layer
966 (BL, surface to 800 hPa) and the total column (TC, surface to 200 hPa) (unit: Gg N) in
967 the INTEX-NA04 simulation (values shown in each cell represent BL/TC values)

Simulations	Species	Emissions[1]	Burden	Dry Deposition[2]	Wet deposition	Net export[3]	Eastward Flux[4]
INTEX-NA04	NO_x	537/723	4/11	80	--	87/33	2/20
	PANs[5]	--	4/16	7	--	23/42	3/55
	HNO_3	--	5/12	101	126/302	64/42	4/29
	Others[6]	--	2/5	47	8/37	-10/18	1/12
	NO_y[7]	537/723	15/44	235	134/339	164/135	10/116
INTEX-NA99	NO_y	694/880	19/49	308	177/406	205/151	10/121
INTEX-NA99-LowLght	NO_y	531/560	15/34	231	127/230	169/90	10/84

968 [1] Emissions include surface, aircraft, biomass burning and lightning sources
969 [2] Dry deposition only applies to the lowest model level
970 [3] Net export is absolute value of the sum of total 3-D advective tendency, convective tendency and the
971 diffusive tendency within the United States
972 [4] Export across the east wall (along 67.5°W longitude line, extending from 24 to 48ºN, from surface to 200
973 hPa); it is included in net export
974 [5] PANs include PAN ($CH_3CO_3NO_2$) and mPAN ($CH_2CCH_3CO_3NO_2$)
975 [6] Other species include oxidized products from NO_x other than HNO_3 and PANs, mainly isoprene nitrates
976 [7] There are < 4% imbalances between the emissions and the sum of deposition and net export within the
977 BL and the TC
978
979

Table 3. July budget of NO_y species in the U.S. (24-48ºN, 127.5-67.5ºW) free troposphere (FT, 800-200hPa)[1] (unit: Gg N)

Experiments / Budget terms		INTEX-NA04-LowLght	INTEX-NA04
FT	Source[1]	203	360
	Burden	19	29
	Deposition	103	205
	Net Export	95	145
	Eastward Export	74	106

[1] We assume that for the FT, the "source" term includes inflow through the west wall (24 Gg N in INTEX-NA04-LowLght , 30 Gg N in INTEX-NA04), BL ventilation (149 GgN in INTEX-NA04-LowLght, 144 GgN in INTEX-NA04) and emissions within the FT (29 Gg N in the INTEX-NA04-LowLght, 186 Gg N in INTEX-NA04, including 15 Gg N from biomass burning and aircraft emissions); the "Net export" term includes northward, southward and eastward export; the "deposition" term includes only the wet deposition since dry deposition only occurs in the model lowest level

990 **Table 4.** Contribution from different components to the total free troposphere (FT) U.S.
991 NO_y export to the North Atlantic in the INTEX-NA04 simulation during July, 2004 (unit:
992 Gg N)

Assumptions[1]	The FT NO_y eastward export[2]	Inflow from the west wall	Lightning increase[3,6]	Original Lightning[4,6]	Biomass burning and aircraft source	Derived lofted surface source[5]
A	106	29	26	0-14	0-15	22-51
B	106	0	32	0-14	0-15	45-74

993 [1] Assumptions: A. NO_y entering through the west wall blows directly across the region and is exported
994 eastward through the east wall; B. NO_y from the west wall is all deposited within the United States.
995 [2] Defined as the eastward NO_y export flux through the east boundary of the United States (24-48N, 67.5W)
996 from the INTEX-NA04 simulation
997 [3] Calculated as the difference between the INTEX-NA04 and INTEX-NA-LowLght simulations, see
998 Section 4.3
999 [4] Original lightning in the INTEX-NA04-LowLght simulation, see Section 4.3
1000 [5] This term is derived as: the FT NO_y eastward export - the other components (inflow from the west wall,
1001 local lightning increase, original lightning, biomass burning and aircraft source)
1002 [6] See calculations in Section 4.3

Figures

Figure 1

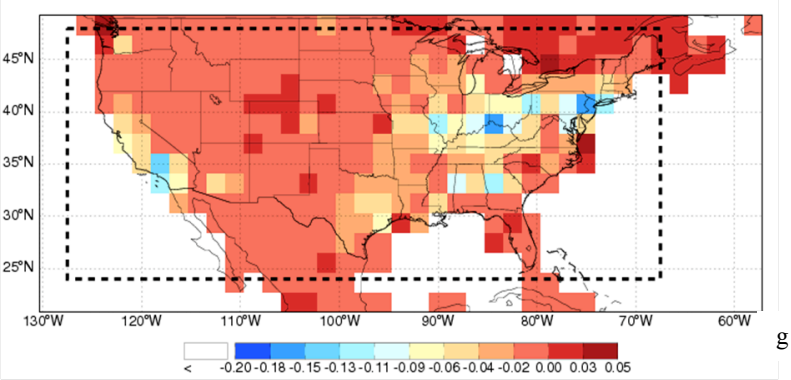

Figure 1. NO_x surface emission change (including anthropogenic and soil emissions). The continental United States boundaries, 24-48ºN, 67.5-127.5ºW, are shown as black dashed lines. Negative value indicates emission decreases from 1999 to 2004

1006 Figure 2

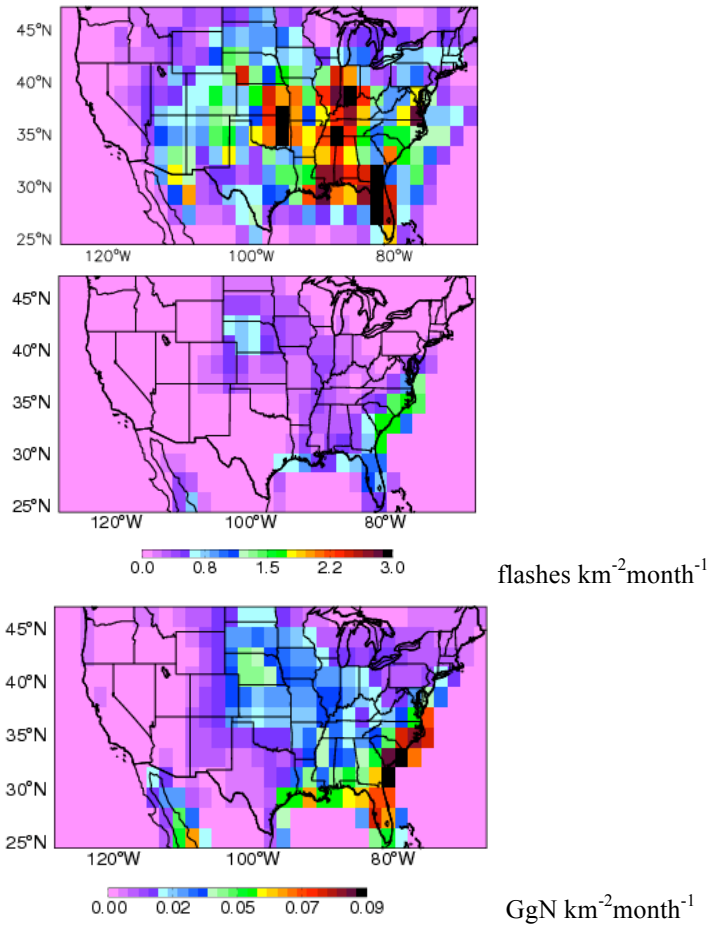

Figure 2. The NLDN observed Cloud-to-ground (CG) flash frequency (a, top), the MOZART-4 simulated CG flash frequency (b, middle) and the lightning NO_x source after adjusting by a factor of 10 to better match the observational constraints (c, bottom) over the contiguous United States (24-48ºN, 67.5-127.5ºW) during July, 2004

1007

1008

1008 Figure 3

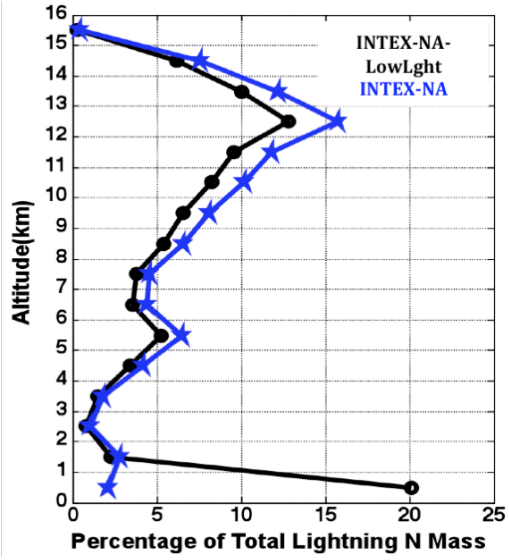

Figure 3. Vertical profiles used for allocating the lightning NO_x source in the INTEX-NA-LowLght (black) and INTEX-NA (blue) simulations (see Table 1 and Section 2 for details).

1009

1010

1010 Figure 4

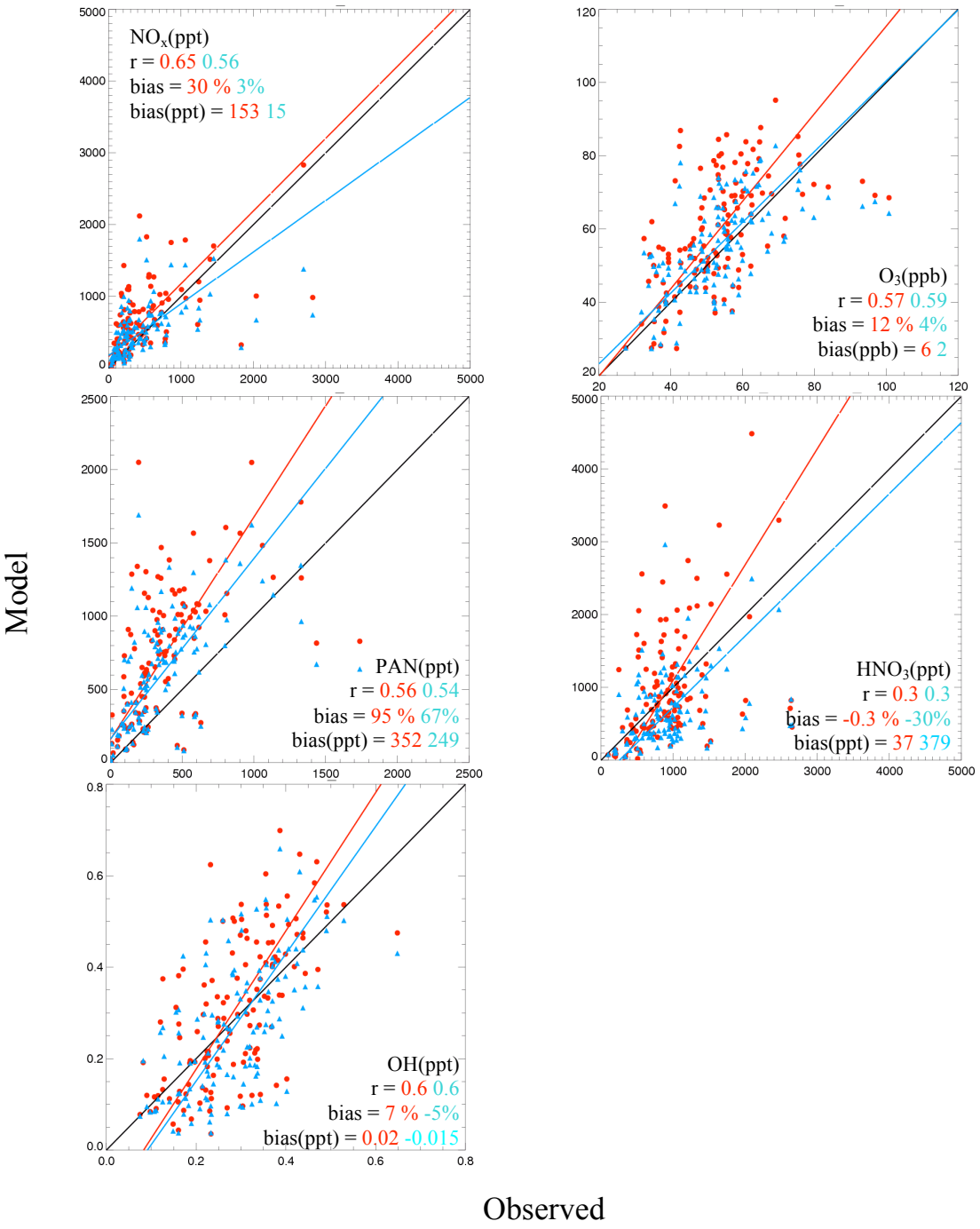

Figure 4. Modeled versus observed concentrations of selected species below 2 km in the eastern United States during INTEX-NA period from the INTEX-NA99 simulation (red) and from the INTEX-NA04 simulation (blue). Model results are sampled every minute along the NASA DC-8 flight tracks in the eastern United States, and then both observations (1 minute average) and model results are averaged onto the model grid. Observations shown from NASA DC-8 are NO_x(a)[calculated as NO + NO_2, PI, *D. Tan*, Georgia Institute of Technology], O_3(b)[PI, *M. Avery*, NASA LaRC], PAN(c)[*Singh*, 2007], HNO_3(d)[PI, R. Talbot, University of New Hampshire] and OH(e)[*Ren et al.*, 2008]; the organic correlation slopes of the INTEX-NA99 and INTEX-NA04 model simulations are shown as red and blue lines respectively; the black

line indicates a line with a 1:1 slope; here and after, to account for the recent corrections to ATHOS absolute calibration [*Ren et al*., 2008], the observed OH was scaled up by a factor of 1.64 for comparison with our model.

1011

1012

1012 Figure 5

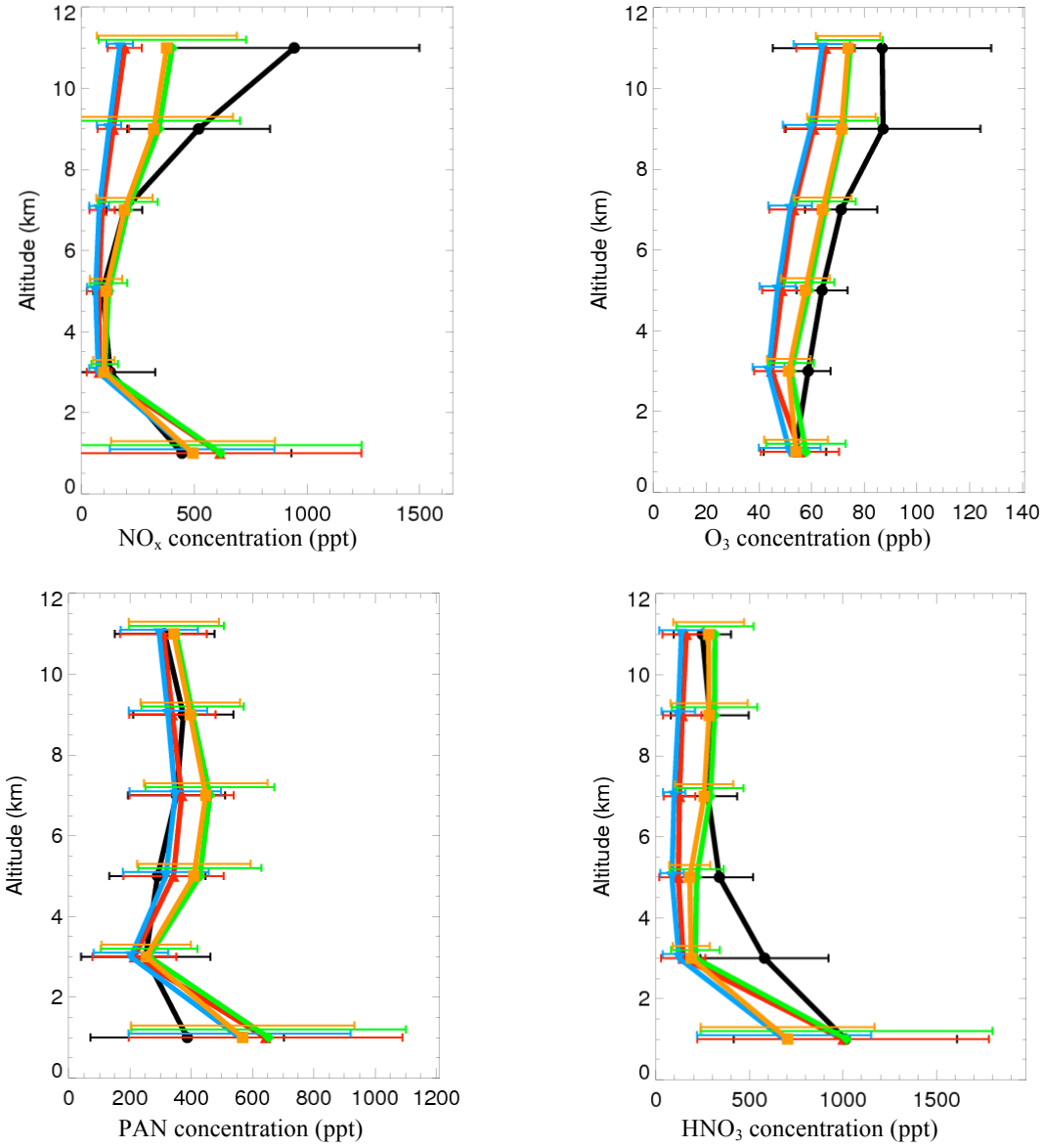

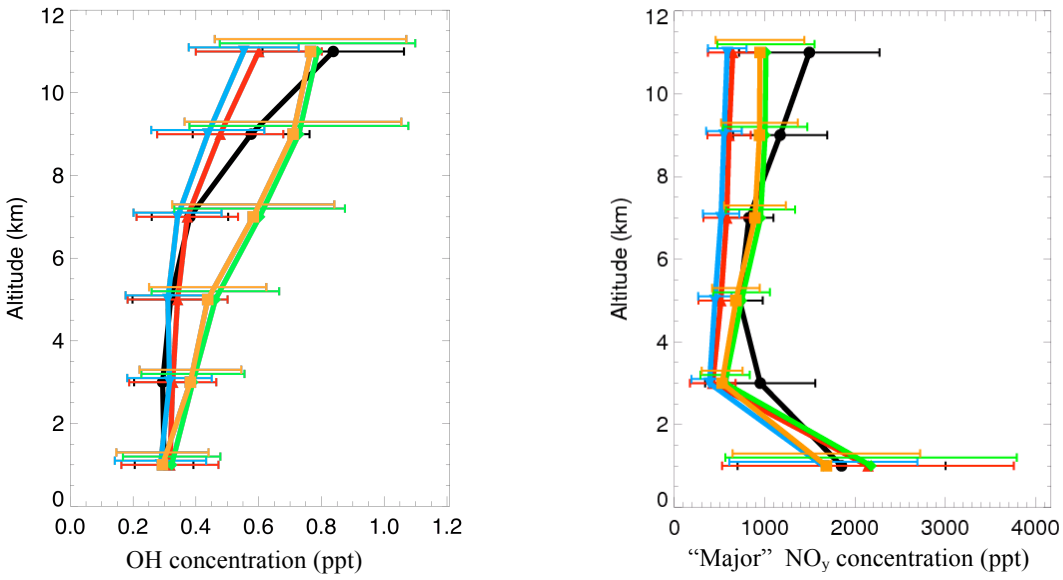

Figure 5. Mean vertical profiles of NO_x (a), O_3 (b), PAN (c), HNO_3 (d), OH (e), and the major NO_y species (f, NO_x, PAN and HNO_3) during the INTEX-NA campaign in July-Aug 2004. Observations from the DC-8 aircraft (black) are compared with the INTEX-NA99-LowLght (red), INTEX-NA04-LowLght (blue), INTEX-NA99 (green) and INTEX-NA04 (orange) simulations. Horizontal bars show the standard deviations of each data set within each 2km layer. Simulated concentrations are sampled every minute along all the flight tracks for comparison with the observations. Both observation and models are then averaged within each horizontal model grid in 2 km altitude bins, and finally these gridded data are averaged (weighted by area) in each layer to get regional mean profiles

1013

1014

1014 Figure 6

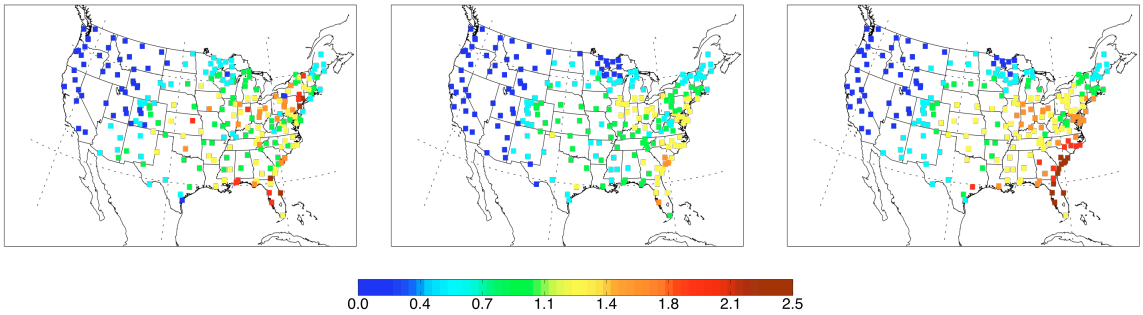

Figure 6. Inorganic nitrate wet deposition (unit: 10^{-1} g N m^{-2}) over the United States (June-August, 2004) from observations (left) and from the INTEX-NA04-LowLght (middle) and INTEX-NA04 (right) simulations (r = 0.75 between model and observed values in both simulations)

1015

1016

1016 Figure 7

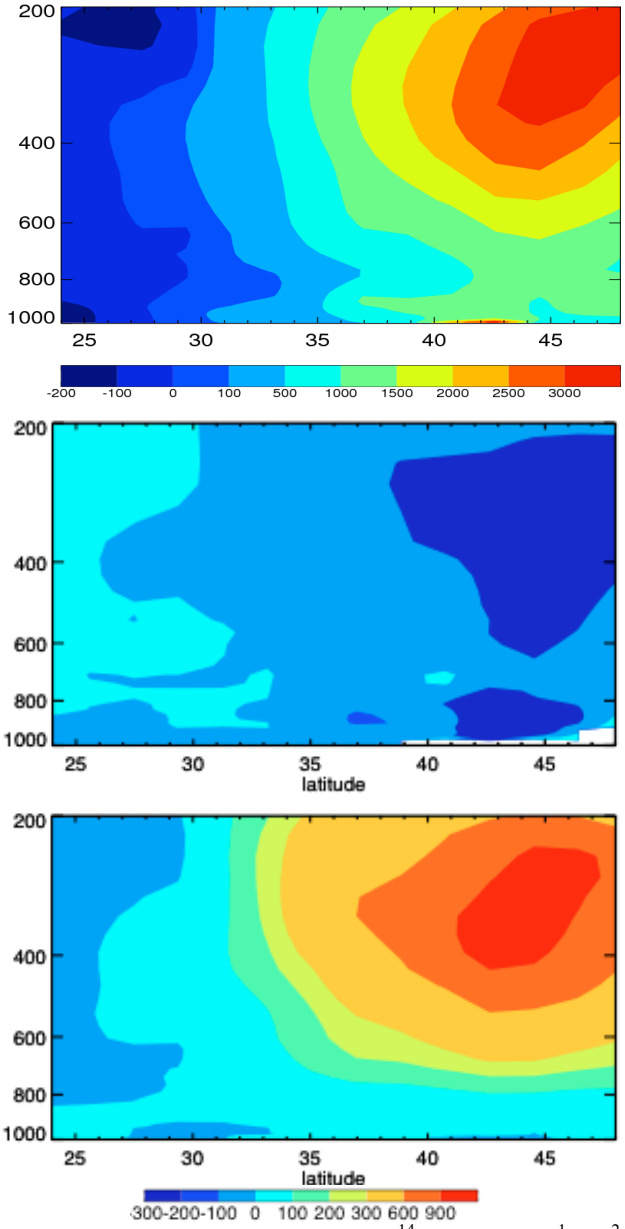

Figure 7. Latitudinal pressure section of NO_y fluxes (unit: 10^{-14} moles N sec^{-1} cm^{-2}) in the INTEX-NA04 simulation (a, top), changes in NO_y fluxes (unit: 10^{-14} moles N sec^{-1} cm^{-2}) through the east wall (67.5ºW) due to the anthropogenic emission regulations (b, middle, fluxes from INTEX-NA04 minus that from INTEX-NA99) and due to lightning adjustment (c, bottom, INTEX-NA04 minus INTEX-NA04-LowLght) through a wall at 67.5ºW, between 24 and 48 ºN during July, 2004; positive values indicate eastward fluxes while negative values indicate westward fluxes.

1017

1018

1018 Figure 8

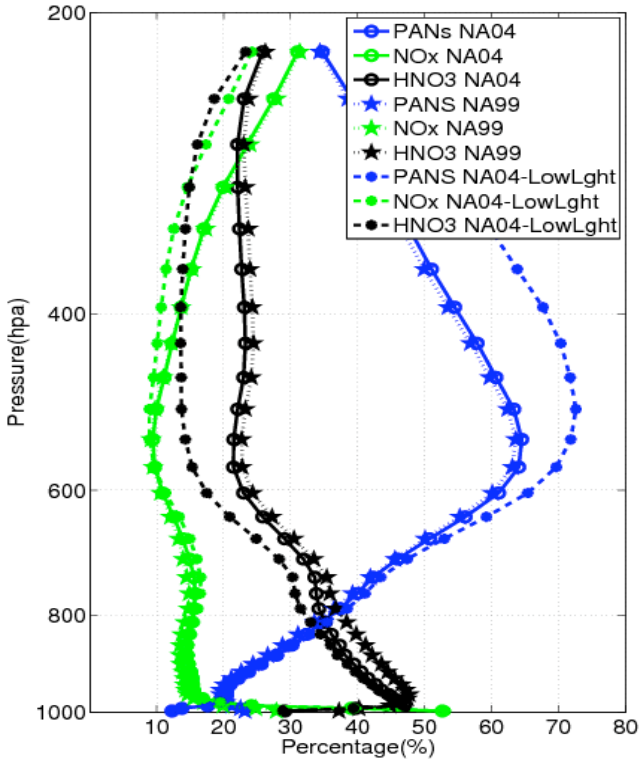

Figure 8. Relative contribution of the major NO_y components to the total NO_y flux through the east wall (67.5ºW, from 24-48ºN) of the United States in the INTEX-NA04 (open circles), the INTEX-NA99 (stars), the INTEX-NA04-LowLght (filled circles) simulations. Simulations are described in Table 1.

1019

1020

1020 Figure 9

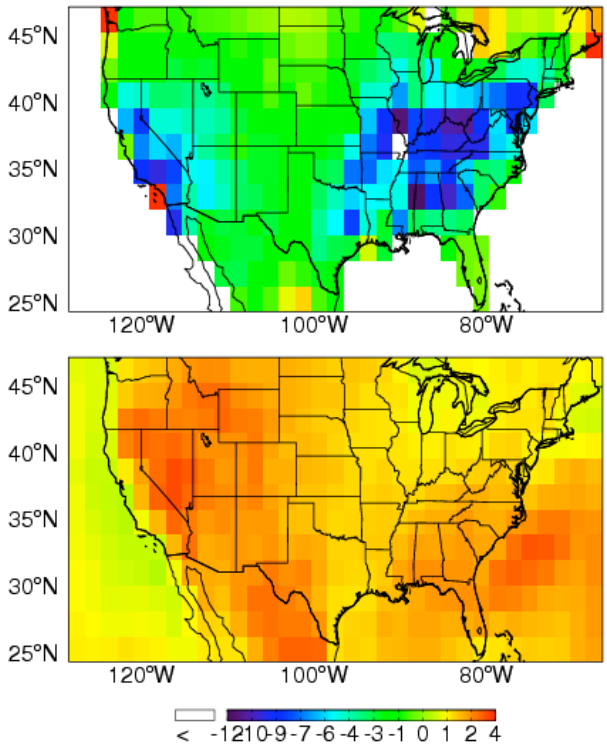

Figure 9. Monthly mean MDA8 O_3 concentration change due to decreases in the U.S. anthropogenic NO_x emissions (top, only land-boxes are shown) and due to increases in lightning NO_x (bottom) (unit: ppbv)

1021